ELSEVIER

Surface Science 482–485 (2001) 1319–1324

SURFACE SCIENCE

www.elsevier.nl/locate/susc

AFM investigation of selective etching mechanism of nanostructured silica

A.A. Bukharaev *, N.I. Nurgazizov, A.A. Mozhanova, D.V. Ovchinnikov

Physics and Chemistry Surface Laboratory, Kazan Physical–Technical Institute, Russian Academy of Sciences, Sibirsky trakt, 10/7, 420029 Kazan, Russian Federation

Abstract

We have developed the atomic force microscope (AFM) for in situ observation of SiO_2 etching in the HF aqueous solution. This work is devoted to the AFM investigation of etching of the SiO_2 surface layer modified by high-dose Fe^+ ion bombardment. Such samples have a two-phase nanostructure (SiO_2 containing buried Fe nanoparticles). Formation and dissociation of nanorelief during etching was observed in situ with AFM. The computer animation of this phenomenon was made with morphing of the experimental AFM images. The additional in situ registration of the optical absorption of Fe nanoparticles during etching, ex situ AFM and ferromagnetic resonance measurements enable us to propose that observed morphology transformation takes place because the etching rate of Fe nanoparticles is much higher than the SiO_2 etching rate. This etching mechanism was used for computer simulation of the AFM image transformation during etching of the model samples with buried nanoparticles. Good correlation of simulated and experimental AFM images and the corresponding surface roughness parameters vs. etching time confirms that this structural model and the mechanism of selective etching are correct.

Keywords: Atomic force microscopy; Etching; Solid–liquid interfaces; Ion bombardment; Surface structure, morphology, roughness, and topography; Computer simulations; Silicon oxides

1. Introduction

The development of the atomic force microscopy (AFM) has given the possibility to obtain a three-dimensional image of surface of solids with the nanometer-scale resolution in liquid and thus to observe the transformation of the surface etching in situ in real time scale [1]. This allows one to obtain the data about the properties both of the surface and the structure of a much deeper surface layer.

The preliminary investigations showed that the selective chemical etching is effective for the study of the multi-phase materials, which have the different etching rates for different phases. Particularly, in that way we have determined the absolute etching rates of silicon dioxide in the HF aqueous solution [2]. The sample consisted of the separate submicron SiO_2 fragments patterned on the Si surface. In Ref. [2] it has been shown that after P^+ ion bombardment the etching rate of SiO_2 increases as the irradiation dose increases, due to radiation defects formed during ion bombardment.

* Corresponding author. Tel.: +7-8432-760563; fax: +7-8432-765075.

E-mail address: bukh@dionis.kfti.knc.ru (A.A. Bukharaev).

0039-6028/01/$ - see front matter
PII: S0039-6028(01)00782-8

Herewith the etching rate increases in five times at a dose of 10^{15} P/cm^2 and does not increase more as the bombardment dose increases.

This paper presents the results of the AFM investigations of in situ and ex situ etching in HF aqueous solutions of fused silica and SiO_2 films. These samples contain iron nanoparticles formed in their undersurface layer by Fe^+ ion bombardment. These materials are of interest because they can be used as media for optical or magnetic recording. The selective chemical etching allows one to obtain the additional data about the structure of the undersurface two-phase layer.

Unfortunately it is not possible to make an unambiguous conclusion about the mechanism of etching of such samples and about the structure of the two-phase undersurface layer on the basis of the analysis of the experimental AFM images only. Thus in this work the optical and ferromagnetic resonance (FMR) measurements have been additionally applied allowing us to control the number of iron nanoparticles in the undersurface layer of the sample.

The computer simulation of the AFM images obtained during the etching of similar model structures provides an essential advance in understanding of physical–chemical processes within the solid–liquid interface. The roughness parameter (RMS) of the surface area imaging by AFM is used as the quantitative parameter describing the kinetics of formation of micro- and nanorelief at etching. The comparison of morphologies of the simulated and experimental AFM images and also of RMS dependences on etching time allows us to test the suggested structural model and the mechanism of the selective etching of the investigated two-phase nanomaterial.

2. Experimental results and discussion

The two types of the samples have been investigated: fused silica (f-SiO_2) and SiO_2 films with thickness of 100 nm formed on crystalline Si substrate (SiO_2–Si). The samples were irradiated by Fe^+ ions with 40 keV energy and at a dose of 0.8×10^{17} Fe/cm^2. The undersurface implanted layer of such samples is a two-phase nanostructure, which consists of silicon dioxide containing the separate α-Fe nanoparticles (α-Fe/SiO_2) [3]. Buried α-Fe metal nanoparticles exhibit the characteristic optical plasmon resonance and the FMR signal. Transmission electron microscopy, Mössbauer spectroscopy, X-ray and electron diffraction were also used to characterize sizes and distribution of buried α-Fe nanoparticles [3]. At dose used the sizes of formed iron nanoparticles distribute from 5 to 100 nm with the aspect ratio of their diameter to the thickness of about 1 for the smallest, almost spherical, particles and of about 2.5 for the biggest ellipsoidal particles. The average lateral distance between the nanoparticles is in the range from 10 to 100 nm. Most of the nanoparticles buried into the undersurface layer on the depth up to 60 nm and protected from above by the thin SiO_2 layer with the thickness of about 5 nm. The data obtained in our previous investigations [3] enabled us to conclude that the surface layer of SiO_2 with α-Fe nanoparticles has the structure schematically presented in Fig. 1a.

The weak HF aqueous solutions with the volume concentration of HF from 0.25% to 0.025%

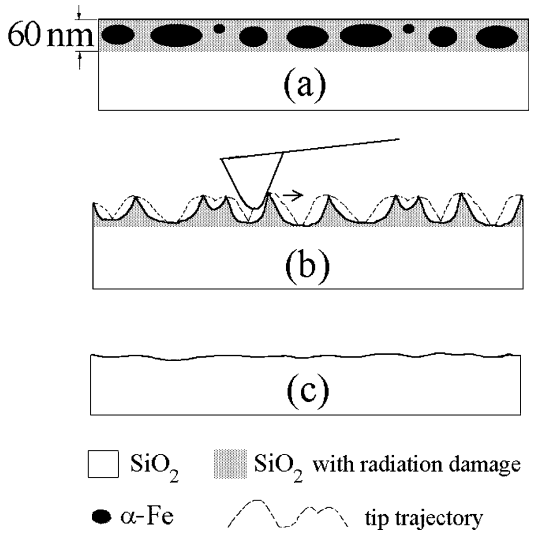

Fig. 1. Cross-sectional scheme of the α-Fe/SiO_2 nanostructure and its selective etching in the HF aqueous solution. (a) Initial stage of the Fe^+ implanted SiO_2. (b) Formation of the nanorelief and the AFM tip trajectory due to the dissolution of α-Fe nanoparticles. (c) Final stage of the etched implanted sample.

were used for chemical etching. The measurements were carried out with a Solver-P4-18RM scanning probe microscope made by Russian firm NT-MDT. The description of the liquid cells used in this work and the respective methods of AFM measurements were published in Ref. [2]. The two types of experiments were carried out: in situ experiments, when the AFM measurements were made in a contact mode directly in the acid solution obtaining the AFM images from the same surface area one-by-one during its chemical modification; and ex situ experiments, when the sample was etched for a certain time at first and afterwards it was removed from the solution, washed in distilled water, dried and then it was measured in air with the AFM working in a tapping mode. The number of α-Fe particles remaining in the SiO_2 surface layer after a certain time of etching was controlled ex situ according to the intensity of the characteristic FMR signal of α-Fe. This signal was measured on a Varian E-12 spectrometer. The number of α-Fe particles remaining after etching in the implanted f-SiO_2 sample was also controlled with an optical spectrophotometer Specord M40 in the wavelength range from 200 to 1000 nm. The optical absorption from α-Fe nanoparticles was measured in situ with a spectrophotometer during etching in the HF aqueous solution of a surface layer of implanted f-SiO_2. The comparative experiments of etching in the HF aqueous solutions of the Fe films with the thickness of 30 nm evaporated in vacuum on fused silica were also carried out.

Fig. 2a presents the AFM image obtained ex situ after partial etching in the HF aqueous solutions of the iron-implanted SiO_2–Si. The characteristic protrusions with the apparent lateral sizes from 50 to 120 nm and height up to 60 nm were formed on

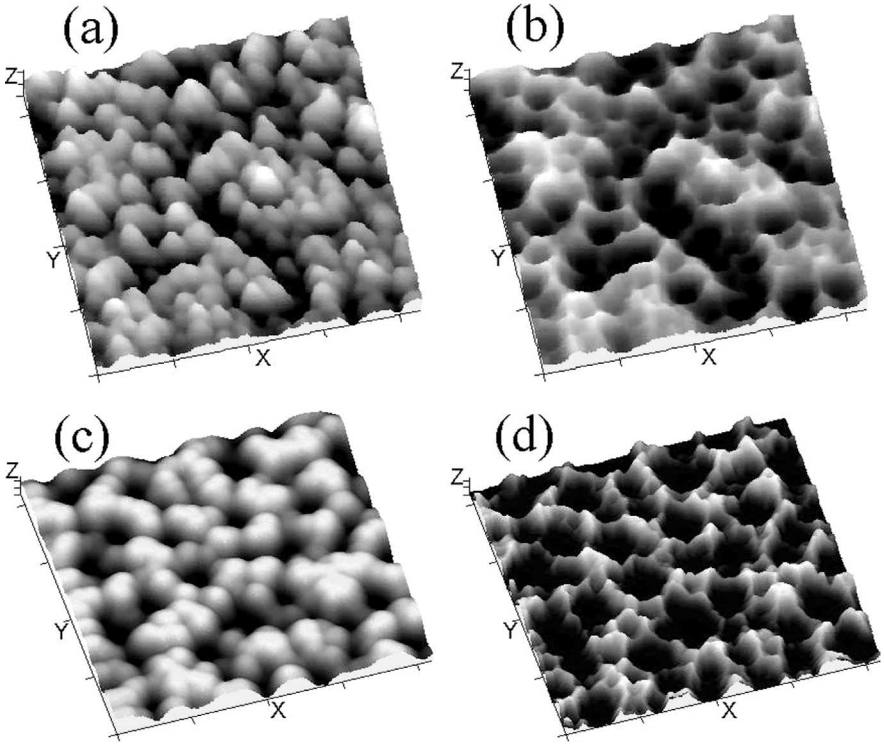

Fig. 2. (a) Experimental AFM image of the partial etched α-Fe/SiO_2 nanostucture and (b) its corresponding deconvoluted AFM image. (d) Simulated surface of the partial etched model α-Fe/SiO_2 nanostucture and (c) its corresponding simulated convoluted AFM image. The image size is 850×850 nm^2. The X and Y scales are 200 nm, and the Z scale is 20 nm.

the SiO_2 surface after etching of such sample during 50 min in 0.025% HF aqueous solutions. At further etching such protrusions disappeared and the surface became relatively smooth again. The same separate nanometer apparent protrusions were formed and then disappeared on the surface of the iron-implanted f-SiO_2 as it dissolved in HF aqueous solutions. The formation and disappearance of such a relief with nanoprotrusions in a real time scale could be observed at in situ etching obtaining the AFM images from the same surface area one-by-one in equal time intervals. Measurements in a relatively weak acid (0.05–0.025% HF) provided up to 40 AFM images from the same area with a scan size 850×850 nm^2 (it took 2 min to obtain one AFM image). It allowed us to create videoclips with computer morphing methods graphically demonstrating the transformation of the surface morphology during dissolution. The appearance and disappearance of the developed nanorelief during etching of f-SiO_2 with buried α-Fe nanoparticles were quantitatively described by the changes of RMS vs. etching time for the same surface area (Fig. 3). For α-Fe/SiO_2, fabricated with 0.8×10^{17} Fe/cm^2 dose, a rather narrow peak demonstrating rapid development and disappearance of the nanorelief was observed (Fig. 3, curve 3).

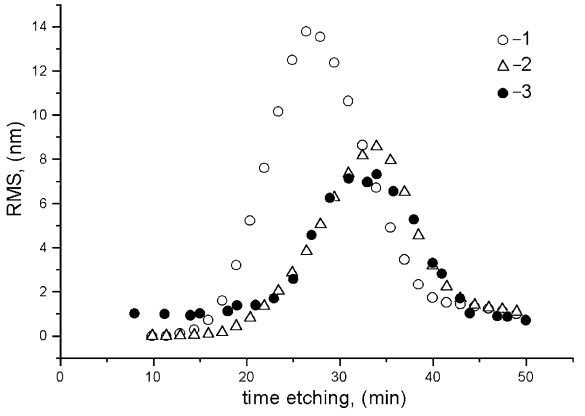

Fig. 3. RMS dependences vs. etching time showing the formation and dissociation of the nanorelief during etching of the 850×850 nm^2 surface area of the model and real α-Fe/SiO_2 nanostucture: (1) model structure, (2) model structure after considering the ''tip–sample'' convolution effect, (3) etching of the real SiO_2–Si sample with buried α-Fe nanoparticles in the 0.025% HF aqueous solution.

The nanorelief formation during etching is obviously associated with the different etching rate of SiO_2 and α-Fe in the HF aqueous solution. However, it is impossible to make an unambiguous conclusion about what is etched faster: SiO_2 or α-Fe (on the basis of AFM measurements only). It can be done if one compares the AFM data with FMR and optical data.

In our previous works on the AFM investigations of SiO_2–Si structures it was shown that the SiO_2 etching rate in 0.25% HF aqueous solution was 0.6 nm/min [2]. After phosphorus irradiation with a dose higher than 10^{15} P/cm^2 the etching rate of the implanted layer in 0.25% HF aqueous solution was 3.5 nm/min. Kinetics of the optical absorption decay from α-Fe studied on a spectrophotometer indicated that in the same HF aqueous solution the dissolution α-Fe nanoparticles buried into SiO_2 dissolved with rate of about the 90 nm/min but the solid iron film on the glass dissolved with the rate of about 200 nm/min. This was much higher than the etching rate of nonimplanted SiO_2 or of SiO_2 containing radiation defects created by P^+ ion bombardment. On the basis of these data it is clear that the nanorelief during etching is formed because iron nanoparticles dissolve much faster than SiO_2. The comparison of the AFM images, optical and FMR data obtained ex situ after etching indicated that α-Fe nanoparticles were absent in the surface layer of the sample at maximal RMS magnitudes. It means that the formation and disappearance of the nanorelief during etching proceed according to the scheme presented in Fig. 1. It should be emphasized that as the AFM tip apex radius ($R_t \cong 30/80$ nm) was comparable with the nanoparticle sizes, the AFM tip movement trajectory was affected by ''tip–sample surface'' convolution effect [4,5]. The size and shape of the experimental tip apex were determined using the special test sample with deconvolution method described in Refs. [4,5]. The test sample was made by lithographic techniques, producing an array of spikes of about 700 nm in height with the apex radius of 10 nm and the cone angle of 20° [6]. The value $R_t \cong 30$ nm was typical for the tip used in the tapping mode and

$R_t \cong 80$ nm for the tip used in the contact mode. Both in contact and in tapping modes the apparent experimental AFM images noticeably differ from real surface morphology due to convolution effect. To reduce the distortions caused by these effects the deconvolution computer method developed earlier [4] was applied. Fig. 1b shows reconstruction of the experimental AFM image by computer deconvolution. It is seen how the original image consisting of the apparent separate protrusions is transformed into the image of pits closely placed to each other. These actual pits were formed after dissolution of the iron nanoparticles. The lateral sizes of such pits are in the range from 40 to 100 nm, their depth is up to 60 nm and the average distance between them is of about 100–150 nm. It is very likely that the observed apparent protrusions in the experimental AFM images are inverted images of the AFM tip apex, which enveloped the very sharp protrusions of etched SiO_2 during scanning. It occurs because the apex radius of these protrusions was smaller than the apex radius AFM tip used in experiment (as it is schematically shown in Fig. 1b).

To verify the mechanism of the formation and the dissociation of the nanorelief during etching of α-Fe/SiO_2 nanostructure the computer simulation of the transformation of the AFM images during etching was carried out as follows. At first, a model of virtual three-dimensional sample representing a matrix with buried iron nanoparticles was created. The algorithm applied to create the model sample was similar to that used in Ref. [7] to simulate the formation of iron nanoparticles obtained by the Fe^+ ion implantation into sapphire. According to this algorithm, the Fe atoms implanted in a crystal lattice form fine particles of α-Fe, the lattice around the particles is deformed tremendously, and many defects and vacancies are produced in the vicinity of particles. Fe atom coming close to a particle is most likely trapped at vacancies to make the particle grow more.

The main fitting parameter for computer simulation is the number of vacancies produced in the vicinity of a particle. Using the trial-and-error method we have created a model two-phase sample for the dose of 10^{17} Fe/cm^2 and the ion energy of 40 keV. Here the buried iron nanoparticle size distribution (from 5 to 120 nm) was very close to the corresponding experimental data.

Then the surface etching of such a model sample was computer simulated under the conditions when the buried nanoparticle etching rate was set to be five times higher than the etching rate of the matrix. The time sequence of simulated three-dimensional images reflecting step by step the transformation of the same surface area during selective etching of the model two-phase nanostructure was obtained. One of such simulated images is presented in Fig. 2d. The RMS surface parameter vs. time etching for such model sample was also obtained (Fig. 3, curve 1). The AFM images of the etched surface differ essentially from the real surface morphology due to the "AFM tip–surface" convolution effect. To consider the influence of this effect the scanning of the surface with the AFM tip during etching was also simulated. The model tip with a half-spherical apex having $R_t = 80$ nm close to one of the above mentioned experimental AFM tip was applied. As an example, Fig. 2c shows the simulated convoluted AFM image obtained from the corresponding surface area presented in Fig. 2d. One can see easily as due to the convolution effect the pits resulting from iron particle etching transform into the apparent protrusions. The corresponding RMS parameter vs. time etching was also obtained (Fig. 3, curve 2).

The visual comparison of these simulated AFM images with the experimental ones demonstrates good qualitative coincidence. Both cases in experiment and in simulations the apparent protrusions in instead of the real pits obtained due to etched iron nanoparticles were observed. The best qualitative coincidence of the morphologies of simulated and experimental AFM images during selective etching was observed in the case when the lateral nanoparticle sizes of the model sample were set in the range of 5–120 nm. These sizes are close to α-Fe nanoparticle sizes obtained with transmission electron microscopy for real SiO_2–Si samples [3].

The RMS vs. time etching was used as a quantitative parameter to compare the experimental and simulated AFM data obtained during etching. The RMS was measured on the same area during etching. That is why the obtained RMS curves

show only the comparative change of the RMS parameter during etching. The simulated and experimental RMS curves differ in shape (Fig. 3, curves 1 and 3) if the convolution effect is not taking into account for the simulated curve. It is essential that after considering the "tip–sample" convolution the form of the simulated RMS curve significantly changes and approaches the experimental one (Fig. 3, curves 1–3). Good coincidence of the simulated and experimental RMS curves confirms that this two-phase nanostructured model sample and the scheme of etching process are correct. On the basis of computer simulations and experimental data it can be concluded that at radiation doses of about 10^{17} Fe/cm^2 the most part of the nanoparticles are buried into the undersurface layer and protected by the SiO_2 layer with thickness of 5–10 nm. Therefore their dissolution in HF aqueous solution begins only after removing this protecting layer.

3. Conclusions

For the first time it is shown that the atomic force microscopy on the basis of in situ selective liquid etching can be successfully used to study the etching of two-phase surface nanostructures. It is demonstrated that to obtain reliable information about the real change of the surface morphology during its etching it was necessary to consider the "AFM tip–surface" convolution effect. The deconvolution method for the surface reconstruction is especially important when the sizes of nanorelief elements formed during etching are comparable with the AFM tip apex size.

The data about the changes of optical and magnetic properties of silicon dioxide implanted by Fe^+ ions allows us to determine that the etching rate of α-Fe nanoparticles buried into SiO_2 far exceeds the etching rate of the matrix (SiO_2 with radiation defects). The model of the two-phase α-Fe/SiO_2 nanostructure fabricated with Fe^+ ion bombardment is suggested. It explains the surface transformation, the changes of its optical and magnetic properties during etching.

The computer AFM simulations shows good coincidence with results of the AFM experiments. It confirms the correctness of the two-phase nanostructured model sample and mechanism of its etching.

Acknowledgements

This work was supported by the Russian of Basic Research Foundation (grant 98-03-32753), the Ministry of Science of Russian Federation (grant 02.04.3.1.40.э.22) and by the NIOKR Foundation of Tatarstan Republic (grant 14-01).

References

[1] D.W. Britt, V. Hlady, Langmur 13 (1997) 1873.
[2] A.A. Bukharaev, N.I. Nurgazizov, A.A. Mozhanova, D.V. Ovchinnikov, Russian Microelectr. 28 (1999) 330.
[3] A.A. Bukharaev, A.V. Kazakov, R.A. Manapov, I.B. Khaibullin, Sov. Phys. Solid State 33 (1991) 578.
[4] A.A. Bukharaev, N.V. Berdunov, D.V. Ovchinninkov, K.M. Salikhov, Russian Microelectr. 26 (1997) 137.
[5] P. Markiewicz, S.R. Cohen, A. Efimov, D.V. Ovichinnikov, A.A. Bukharaev, Probe Microsc. 1 (1999) 355.
[6] V. Bykov, A. Gologanov, V. Shevyakov, Appl. Phys. A 66 (1998) 499.
[7] T. Kobayashi, A. Nakanishi, K. Fukumura, J. Radioanal. Nucl. Chem. 239 (1999) 313.